Journal of The Electrochemical Society, **155** (11) J297-J300 (2008)
0013-4651/2008/155(11)/J297/4/$23.00 © The Electrochemical Society

Microarrayed Nanostructured Titania Thin Films Functionalized for Hydrogen Detection

A. J. Monkowski,[a,z] A. Morrill,[b] and N. C. MacDonald[c]

[a]*Department of Materials Science and Engineering,* [b]*Department of Chemistry and Bioscience, and* [c]*Department of Mechanical Engineering, Department of Materials, University of California, Santa Barbara, Santa Barbara, California 93106, USA*

Wafer scale arrays of nanostructured titania (NST) sensing elements have been fabricated using standard microfabrication techniques. Sensing elements are 20 μm on a side and formed by the oxidation of titanium thin films in aqueous hydrogen peroxide. NST elements are highly sensitive to oxygen, but only slightly sensitive to hydrogen. High sensitivity to hydrogen is achieved by modification of the sensors with platinum. A platinum salt solution is introduced to the NST sensor elements and subsequently thermally decomposed. When exposed to 10 mT of hydrogen at 250°C, the functionalized devices exhibit over a one-order-of-magnitude resistance decrease with a response time of ~7 s; conversely, unmodified NST exhibit little, if any, response under the same conditions. Proposed sensing mechanisms of the NST elements are briefly discussed.
 [DOI: 10.1149/1.2969284]

Manuscript submitted April 2, 2008; revised manuscript received June 18, 2008. Published September 5, 2008.

An ongoing effort in chemical sensor research is the miniaturization of devices. One approach to achieving this goal is the use of nanostructured materials as the sensing element; their high surface-to-volume ratio can yield very sensitive devices with micron-scale footprints. Metal oxides have proven to be a good candidate for this application due to their established functionality as a sensing platform and the numerous existing routes to their formation in a nanostructured configuration. With regard to titania, thin films of nanorods, nanotubes, and inverse opal structures have been formed by electrospinning, anodic oxidation, and templating methods, respectively.[1-3]

Titania was first investigated as a chemical sensor for the monitoring of oxygen in automobile exhaust. Research on these lambda sensors focused on the rutile phase of titania due to the stability of this phase in the high-temperature operating environments of an exhaust sensor.[4] More recently, the anatase phase of titania has received considerable attention as a gas-sensing material. Anatase has a less dense crystal structure, and studies on both bulk single crystals and sputtered thin films have shown that the Hall mobility in the anatase phase is one to three orders of magnitude greater than in the rutile phase. Studies also found that the mobility was n-type and carriers are generated thermally from shallow donor sites arising from oxygen vacancies.[5,6] Anatase titania has been shown to be sensitive to O_2, H_2, and C_2H_4, in porous ceramic, thin-film, and nanostructured arrangements.[1,7-11]

One method of forming nanostructured titania (NST) is to oxidize metallic titanium in a hydrogen peroxide solution.[12] Recently, members of our group developed processes to integrate this method of NST formation with standard microfabrication techniques to create arrays of micron-scale, individually addressable nanostructured thin films.[13] These devices, which were annealed to form the anatase phase, exhibited a two-order-of-magnitude resistance increase when exposed to millitorr levels of oxygen at 200°C.[11] Because these thin films are microlithographically defined, large arrays of individually addressable sensors can be fabricated. Developing a scheme to functionalize these microarrayed sensors to facilitate analyte sensitivity and selectivity will offer a platform for a multiplexed, electronic nose-type sensor. Citing that titania, as well as other metal oxide gas sensors exhibit improved hydrogen sensitivity when doped with platinum,[14,15] modification of the NST sensors with platinum is investigated to realize hydrogen sensitivity.

Experimental

Fabrication methods.— Prior to this work, fabrication of arrayed NST-sensing elements was preformed on small substrates (~2 cm^2). This process was modified for this study to facilitate fabrication on the wafer scale, both to achieve higher throughput and to investigate the feasibility of a batch fabrication process for production.

One micrometer of SiO_2 was grown by wet oxidation at 1100°C on 100 mm, n–type silicon wafers; then, 500 nm of titanium was deposited on the wafer using electron beam evaporation. The titanium deposition rate can affect the ultimate microstructure of the NST, so the deposition rate was maintained at 2.5 Å/s for all samples. The film was patterned using a photoresist liftoff process to produce isolated squares. Following this, 250 nm of SiO_2 was deposited by plasma-enhanced chemical vapor deposition, patterned, and etched in a CF_4 plasma to reveal the underlying titanium squares. The oxide film was patterned to slightly overlap the edge of the titanium squares and protect the interface between the thermal oxide and titanium during the oxidation process. The wafer was then placed in a 10% H_2O_2 solution that had been heated to 83°C and left undisturbed in solution for 15 min. The temperature of the solution was monitored using a glass-coated resistive temperature detector probe and kept within 2°C of the target temperature. After removal from solution the sample was rinsed in a deionized (DI) water bath and carefully dried. The samples were then annealed in air at 400°C for 8 h. Ti/Au contacts are deposited and patterned using a liftoff process. The process flow is shown in Fig. 1. The wafer was then diced into samples of ~1 cm^2. A scanning electron microscope (SEM) image of one sensing element is shown in Fig. 2; each sample contains 45 elements.

Platinum modification.— Subsequent to annealing the NST, platinum was introduced to the sensor elements. The desired morphology of the platinum was one in which a minimum amount of platinum was used to conformally cover the TiO_2 while not forming an electrically continuous film. Several techniques were investigated for this application, including physical vapor deposition, photoassisted deposition from solution, and infusion-decomposition methods. The best results were obtained from infusion and subsequent thermal decomposition of H_2PtCl_6 dissolved in 2–propanol. Using a micropipette, 1 μL of 5 mM H_2PtCl_6 solution was placed on a 1 cm^2 sample and allowed to wet the surface. The sample was dried in air for 5 min until the 2–propanol has completely evaporated, and was then heated to 400°C in air for 15 min to thermally decompose the platinum salt and liberate any remaining solute and chlorine. Solution volume and concentration were optimized to produce the desired nanoparticle morphology.

Following oxidation of the NST in hydrogen peroxide, the structure of the sensor was comprised of disordered amorphous walls or wires, ~25 nm in width, connected to form pores with diameters of 100–200 nm. Subsequent to annealing, X-ray diffraction measurements verified the presence of the anatase phase; the rutile phase

[z] E-mail: amonkow@gmail.com

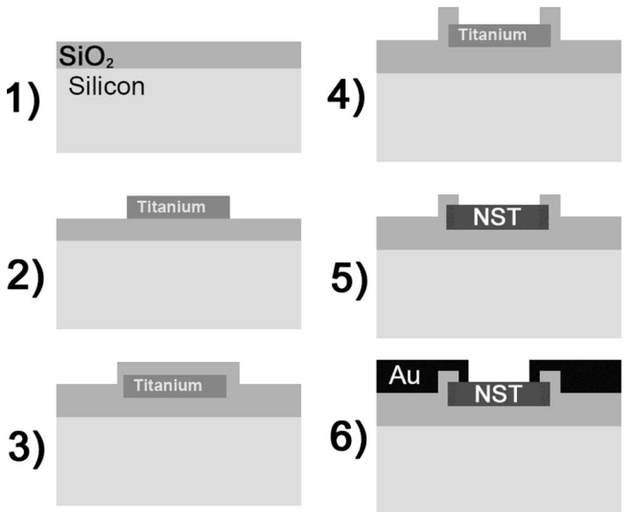

Figure 1. Oxide is grown on a silicon substrate. (2) Titanium is patterned via liftoff. (3, 4) PECVD SiO_2 is deposited and patterned. (5) The sample is oxidized in H_2O_2 solution and annealed at 400°C. (6) Ti/Au electrodes are deposited.

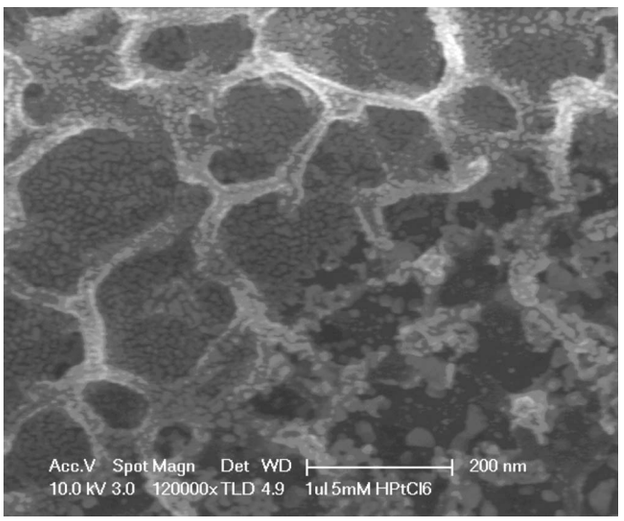

Figure 3. Platinum deposition is carried out by the thermal decomposition of H_2PtCl_6 in 2–propanol. The platinum particle size ranges from 5 to 20 nm in well-covered areas and is larger, up to 50 nm, where platinum coverage is incomplete and non-uniform.

was not observed. Figure 3 shows a SEM image of the NST following platinum deposition; the platinum deposition is conformal, with platinum particles of 5 to 20 nm in size completely covering the observable surface. As shown in Fig. 3, there are some areas in which the platinum coverage was reduced. This was possibly a result of insufficient platinum concentration in solution or ambient moisture interfering with the deposition process. The total amount of platinum deposited averaged across the 1 cm^2 sample corresponded to less than one monolayer of platinum ($\sim$1 $\mu g/cm^2$). It is important to note that the platinum loading was not high enough to form a continuous layer; the sensor electrodes remained electrically isolated.

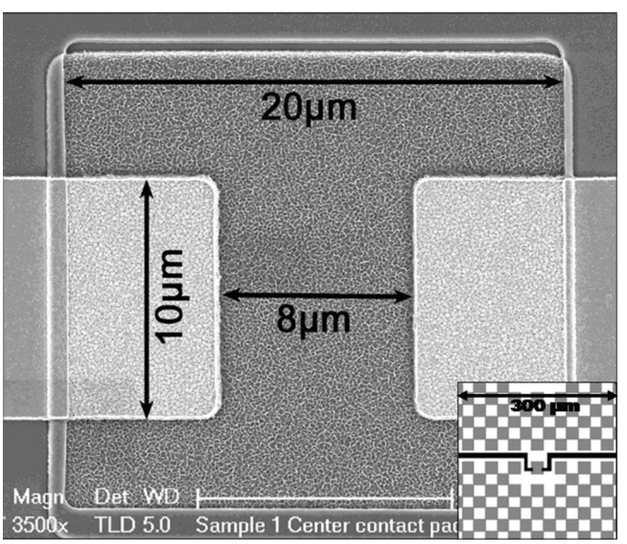

Figure 2. Electrode width and separation is 10 and 8 μm, respectively. The sensing element is 20 μm on a side. Surrounding the sensor is an insulating SiO_2 film. The lower right corner shows a diagram of the element array geometry in which black lines are contacts/wires; gray squares are NST features and white areas are SiO_2 surfaces.

Sensor characterization.— Characterization of the sensor was carried out in a vacuum chamber evacuated to 10^{-4} M Torr prior to testing. The sample was heated using resistive heaters installed in a copper stage. Power and temperature control were provided through a closed-loop control circuit; input for the feedback loop was from a type-K thermocouple. The target and carrier gas (N_2) were injected at a controlled rate through separate mass flow controllers such that the concentration of the target gas could be controlled. A butterfly valve was installed downstream of the chamber to allow for control of the chamber pressure while gas was flowing in the system.

Results

Hydrogen sensing results.— Figure 4 shows the response of the platinum-modified sensors when cycled between nitrogen and a hydrogen/nitrogen mixture at 200°C. Under these conditions, the sensors exhibited a large and rapid resistance decrease. The response time was 10–12 s; recovery time is notably longer than response

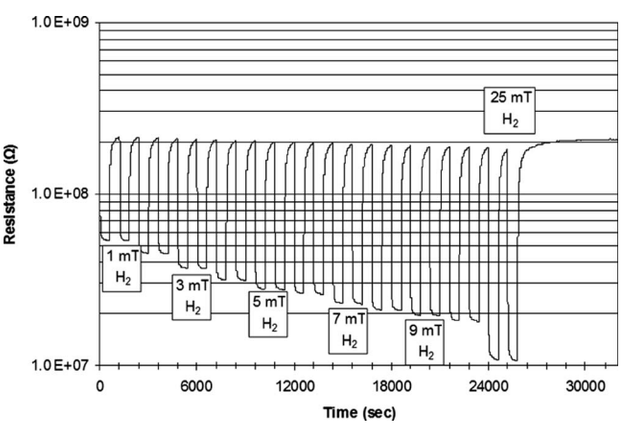

Figure 4. Platinum–modified NST sensing of hydrogen. Testing is carried out at 200°C in a nitrogen environment. The chamber pressure and gas flow are maintained at 500 mT and 25 sccm, respectively. Hydrogen is introduced to the chamber at partial pressures varying from P_H = 1–10 mT in 1 mT increments and ultimately at 25 mT. Hydrogen is cycled on and off in 1200 s increments and two cycles are performed at each P_H.

Table I. Device comparison.

	Bare NST	Pt-modified NST
O_2 Response time (s) (1 mT, 200°C)	48[a]	300
O_2 Response Magnitude 10 log(R/R_0)	17.8	12.3
H_2 Response time (s) (1 mT, 250°C)	600	7
H_2 Response Magnitude 10 log(R/R_0)	−0.14	−6.0

[a] Ref. 11.

time, possibly due to residual hydrogen in the chamber or present in the sample. As higher partial pressures of hydrogen were introduced to the chamber, the 10 min recovery time was not long enough for the sensor to fully recover; however, at the end of the cycling, the initial resistance was restored.

Sensor selectivity.— Because the success of a sensor relies on sensitivity as well as selectively, the response of both unmodified and functionalized sensors were measured in both oxygen and hydrogen environments. Sensor response magnitudes and times are listed in Table I. Modifying the NST sensors with platinum reduced the previously reported O_2 response magnitude and increased the response time by a factor of 6. However, the platinum-modified elements exhibited a H_2 response that was much larger in magnitude compared to the unmodified sensors. Additionally, modified NST sensors exhibited a response time that was two orders of magnitude faster. A comparison of the two responses to hydrogen is shown in Fig. 5.

Hydrogen sensitivity in the Pt/TiO_2 system was a result of hydrogen spillover, in which hydrogen species adsorbed on the platinum surface diffused onto the titania support.[16] These spilt-over hydrogen species acted as an electron donor on the surface of the titania, increasing n-type conductivity.[17] The relatively quick response time observed in this study is attributed to the fine structure of the platinum particles, which are separated, on average, by only tens of nanometers. In this arrangement, the whole of the titania surface quickly reached equilibrium hydrogen coverage due to the short distance the spilt-over species must travel.

The reduced O_2 sensing response of the platinum modified elements was a consequence of reduced titania surface area due to platinum loading. Conduction across the NST sensing element occurred as a result of oxygen vacancies that act as shallow donor sites. When heated in vacuum, anatase titania evolved weaklybound surface oxygen at 125, 190, and 250°C, the latter of these evolutions being the smallest of the three.[18] At the characterization temperature, 200°C, the film lost a majority of the oxygen available for desorption; when O_2 was reintroduced to the environment, it filled some of these sites and reduced the carrier concentration. Platinum surface modification reduced the area available for oxygen adsorption/desorption, decreasing sensitivity. However this did not offer complete insight into the substantially increased O_2 response time of the platinum modified sensors; this could be the result of a surface contamination species introduced during the platinum deposition, which reduced the strength of the titanium–adsorbed oxygen interaction. When a platinum modified sample was exposed to oxygen for 10 min and subsequently exposed to hydrogen within 60 s (i.e., during the recovery time of the sensor), the response time and ultimate resistance value were not affected by the preceding oxygen exposure, suggesting that the sensing mechanism remains a surface effect; oxygen diffusing into the Ti–Pt interface was not a significant response mechanism.

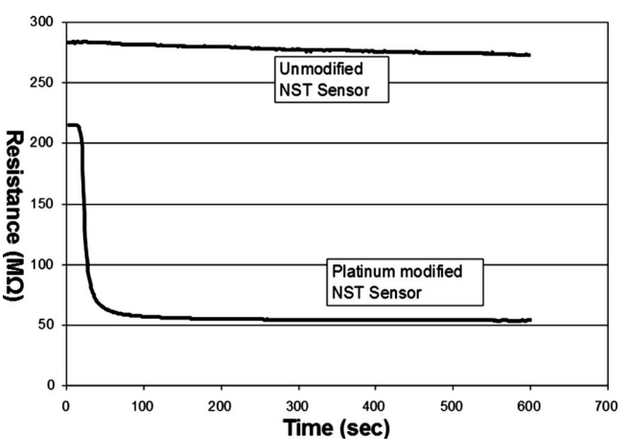

Figure 5. The response of NST sensors with and without platinum modification. At t = 20 s, 1.0 mT hydrogen partial pressure is introduced to the chamber in a nitrogen background. Total pressure is 500 mT and device temperature is 200°C.

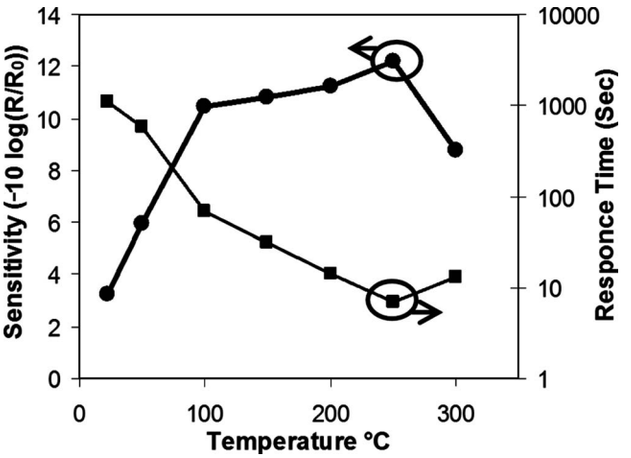

Figure 6. Device performance vs temperature. The device response to 10 mT hydrogen at various temperatures.

Temperature response.— Figure 6 shows sensing behavior at temperatures ranging from room temperature to 300°C. Sensitivity and response time were both optimized at a temperature of 250°C. The initial resistance of the sensor was governed by the number of thermally generated carriers. Upon hydrogen exposure, the resistance decreased as additional carriers were introduced by adsorbed hydrogen. The sensitivity of the device would be improved if the number of hydrogen-generated carriers was increased, and diminished if the number of thermally generated carriers was increased. The latter was the case as temperature was increased from 250 to 300°C. At 300°C, the initial resistance of the sensor was reduced one order of magnitude due to a dramatic increase in thermally generated carriers, diminishing the relative effect of the hydrogen-generated carriers and decreasing sensitivity. At temperatures of $<$250°C, sensitivity decreased with temperature. This was not expected because hydrogen adsorption on platinum should not decrease in this temperature regime. One possible explanation for this behavior is poisoning of the platinum with carbon monoxide, which adsorbs strongly on platinum and can block the adsorption of other species.[19,20] Because testing was done under only rough vacuum, trace amounts of carbon monoxide were present. As the temperature was increased, carbon monoxide desorbs, allowing for increased hydrogen adsorption; temperature-programmed desorption studies of platinum nanoparticles supported on anatase TiO_2 confirm that carbon monoxide desorption occurs between 100 and 200°C,[21] the temperature regime in which the hydrogen response was im-

proved. Also at higher temperatures, the quick initial response was followed by a smaller but much longer resistance decrease, the result of a substantial direct hydrogen-titania interaction contributing to the overall signal, resulting in a longer overall response time. The high performance of the sensor at 200°C is promising because this is the temperature at which unmodified NST oxygen sensors are optimized, suggesting these two sensors could be operated in close proximity, onchip.

Conclusions

Microfabricated NST is a promising platform for fabricating gas sensors. Production of small, high-surface-area sensing elements using a batch-fabrication technique could lead to inexpensive sensors, integrated into common electronic devices. Surface modification via solution methods, such as thermal decomposition of a metal salt, offers an inexpensive route to expanding the selectivity of the NST sensors. We show that modification of NST with platinum yields a sensor with a rapid and large amplitude response upon exposure to hydrogen. As additional surface modifications with metals and metal oxides are investigated and further sensitivities are uncovered, microfabricated NST could offer a promising route to a multiplexed gas sensor.

Acknowledgments

The authors acknowledge Klas Andersson for insightful discussions on the subject of physical chemistry.

University of California, Santa Barbara assisted in meeting the publication costs of this article.

References

1. G. K. Mor, O. K. Varghese, M. Paulose, K. G. Ong, and C. A. Grimes, *Thin Solid Films*, **496**, 42 (2006).
2. P. R. Somani, C. Dionigi, M. Murgia, D. Palles, P. Nozar, and G. Ruani, *Sol. Energy Mater. Sol. Cells*, **87**, 513 (2005).
3. M. Y. Song, D. K. Kim, K. J. Ihn, S. M. Jo, and D. Y. Kim, *Nanotechnology*, **15**, 1861 (2004).
4. T. Y. Tien, H. L. Stadler, E. F. Gibbons, and P. J. Zacmanidis, *Am. Ceram. Soc. Bull.*, **54**, 280 (1975).
5. L. Forro, O. Chauvet, D. Emin, L. Zuppiroli, H. Berger, and F. Levy, *J. Appl. Phys.*, **75**, 633 (1994).
6. H. Tang, K. Prasad, R. Sanjines, P. E. Schmid, and F. Levy, *J. Appl. Phys.*, **75**, 2042 (1994).
7. L. D. Birkefeld, A. M. Azad, and S. A. Akbar, *J. Am. Ceram. Soc.*, **75**, 2964 (1992).
8. G. C. Mather, F. M. B. Marques, and J. R. Frade, *J. Eur. Ceram. Soc.*, **19**, 887 (1999).
9. N. Savage, B. Chwieroth, A. Ginwalla, B. R. Patton, S. A. Akbar, and P. K. Dutta, *Sens. Actuators B*, **79**, 17 (2001).
10. H. Tang, K. Prasad, and R. Sanjines, F. Levy, *Sens. Actuators B*, **26**, 75 (1995).
11. A. S. Zuruzi, A. Kolmakov, N. C. MacDonald, and M. Moskovits, *Appl. Phys. Lett.*, **88**, 102904 (2006).
12. J. M. Wu, S. Hayakawa, K. Tsuru, and A. Osaka, *Scr. Mater.*, **46**, 101 (2002).
13. A. S. Zuruzi, *Integration of Nanostructure Titania into Microsystems*, UC Santa Barbara, Santa Barbara (2005).
14. S. J. Ippolito, S. Kandasamy, K. Kalantar-zadeh, and W. Wlodarski, *Sens. Actuators B*, **108**, 154 (2005).
15. A. S. Ryzhikov, A. N. Shatokhin, F. N. Putilin, M. N. Rurayantseva, A. M. Gaskov, and M. Labeau, *Sens. Actuators B*, **107**, 387 (2005).
16. U. Roland, T. Braunschweig, F. Roessner, *J. Mol. Catal. A: Chem.*, **127**, 61 (1997).
17. U. Roland, R. Salzer, T. Braunschweig, F. Roessner, and H. Winkler, *J. Chem. Soc., Faraday Trans.*, **91**, 1091 (1995).
18. M. Iwamoto, Y. Yoda, N. Yamazoe, and T. Seiyama, *J. Phys. Chem.*, **82**, 2564 (1978).
19. P. Waszczuk, G. Q. Lu, A. Wieckowski, C. Lu, C. Rice, and R. I. Masel, *Electrochim. Acta*, **47**, 3637 (2002).
20. J. J. Baschuk and X. G. Li, *Int. J. Energy Res.*, **25**, 695 (2001).
21. H. Iida and A. Igarashi, *Appl. Catal., A*, **298**, 152 (2006).